J|A|C|S
ARTICLES
Published on Web 04/03/2007

Photosensitive Function of Encapsulated Dye in Carbon Nanotubes

Kazuhiro Yanagi,*,† Konstantin Iakoubovskii,† Hiroyuki Matsui,‡ Hiroyuki Matsuzaki,‡ Hiroshi Okamoto,‡ Yasumitsu Miyata,§ Yutaka Maniwa,§ Said Kazaoui,† Nobutsugu Minami,† and Hiromichi Kataura†

Contribution from the National Institute of Advanced Industrial Science and Technology (AIST), Ibaraki 305-8562, Japan, Department of Advanced Materials Science, The University of Tokyo, Chiba 277-8561, Japan, and Department of Physics, Tokyo Metropolitan University, Tokyo 192-0397, Japan

Received October 13, 2006; E-mail: k-yanagi@aist.go.jp

Abstract: Single-wall carbon nanotubes (SWCNTs) exhibit resonant absorption localized in specific spectral regions. To expand the light spectrum that can be utilized by SWCNTs, we have encapsulated squarylium dye into SWCNTs and clarified its microscopic structure and photosensitizing function. X-ray diffraction and polarization-resolved optical absorption measurements revealed that the encapsulated dye molecules are located at an off center position inside the tubes and aligned to the nanotube axis. Efficient energy transfer from the encapsulated dye to SWCNTs was clearly observed in the photoluminescence spectra. Enhancement of transient absorption saturation in the S1 state of the semiconducting SWCNTs was detected after the photoexcitation of the encapsulated dye, which indicates that ultrafast (<190 fs) energy transfer occurred from the dye to the SWCNTs.

I. Introduction

Functionalization of single-wall carbon nanotubes (SWCNTs) allows one to enhance their electronic properties and is therefore extremely important for their applications.[1] There are two main functionalization strategies: one is to modify the outer surface of SWCNT with organic compounds, such as proteins, DNA, etc.,[2−6] and the other is to encapsulate molecules or metallic atoms inside the nanotube.[7−11] The first route is relatively easy as there are no obvious restrictions to the size, position, and arrangement of the attached molecule. As a result, numerous successful outer-shell functionalizations have been reported. However, this approach inevitably causes undesirable side effects such as creation of defects and loss of the unique one-dimensional (1-D) structure of the SWCNTs, both of which lead to the concomitant decrease in the electrical conductivity.[12] On the contrary, SWCNT functionalization via encapsulation is free from these drawbacks and is therefore beneficial for tuning the physical properties of SWCNTs without losing their unique structure.

Several functionalization techniques utilizing the inner space of SWCNTs have been proposed. Most of them focus on manipulating the conductivity of the SWCNTs using alkali metals, TCNQ molecules, etc.[11,13] However, recently, generation and detection of light by a single SWCNT have been reported, opening the important applications of SWCNTs in nano-optoelectronics.[14−16] Development of techniques that can control the optical properties of SWCNTs has great significance for those applications. The optoelectronic properties of SWCNTs are limited by the absorption spectrum of semiconducting SWCNTs (s-SWCNTs). Changing the nanotube diameter allows one to modify those properties; however, such diameter control is yet a complex technological problem. Development of another methodology that can tune the optical properties of SWCNTs is clearly required.

Photosensitization is a promising technique that can expand the spectral range of light absorption. Therefore, in this study,

† AIST.
‡ The University of Tokyo.
§ Tokyo Metropolitan University.

(1) Kuzmany, H.; Kukovecz, A.; Simon, F.; Holzweber, M.; Kramberger, C.; Pichler, T. *Synth. Met.* **2004**, *141*, 113−122.
(2) Baskaran, D.; Mays, J. W.; Zhang, X. P.; Bratcher, M. S. *J. Am. Chem. Soc.* **2005**, *127*, 6916−6917.
(3) Chen, R. J.; Zhang, Y.; Wang, D.; Dai, H. *J. Am. Chem. Soc.* **2001**, *123*, 3838−3839.
(4) Heller, D. A.; Jeng, E. S.; Yeung, T.; Martinez, B. M.; Moll, A. E.; Gastala, J. B.; Strano, M. S. *Science* **2006**, *311*, 508−511.
(5) Strano, M. S.; Dyke, C. A.; Usrey, M. L.; Barone, P. W.; Allen, M. J.; Shan, H.; Kittrell, C.; Hauge, R. H.; Tour, J. M.; Smalley, R. E. *Science* **2003**, *301*, 1519−1522.
(6) Sun, Y.; Fu, K.; Lin, Y.; Huang, W. *Acc. Chem. Res.* **2002**, *35*, 1096−1104.
(7) Khlobystov, A. N.; Britz, D.; Briggs, G. A. *Acc. Chem. Res.* **2005**, *38*, 901−909.
(8) Monthioux, M. *Carbon* **2002**, *40*, 1809−1823.
(9) Takenobu, T.; Takano, T.; Shiraishi, M.; Murakami, Y.; Ata, M.; Kataura, H.; Achiba, Y.; Iwasa, Y. *Nat. Mater.* **2003**, *2*, 683−688.
(10) Yanagi, K.; Miyata, Y.; Kataura, H. *Adv. Mater.* **2006**, *18*, 437−441.
(11) Izumida, T.; Jeong, G.; Neo, Y.; Hirata, T.; Hatakeyama, R.; Mimura, H.; Omote, K.; Kasama, Y. *Jpn. J. Appl. Phys.* **2005**, *44*, 1606−1610.
(12) Kamaras, K.; Itkis, M. E.; Hu, H.; Zhao, B.; Haddon, R. C. *Science* **2003**, *301*, 1501−1501.
(13) Shiraishi, M.; Nakamura, S.; Fukao, T.; Takenobu, T.; Kataura, H.; Iwasa, Y. *Appl. Phys. Lett.* **2005**, *87*, 093107−093109.
(14) Freitag, M.; Martin, Y.; Misewich, J. A.; Martel, R.; Avouris, P. *Nano Lett.* **2003**, *3*, 1067−1071.
(15) Chen, J.; Perebeinos, V.; Freitag, M.; Tsang, J.; Fu, Q.; Liu, J.; Avouris, P. *Science* **2005**, *310*, 1171−1174.
(16) Misewich, J. A.; Martel, R.; Avouris, P.; Tsang, J.; Heinze, S.; Tersoff, J. *Science* **2003**, *300*, 783−786.

10.1021/ja067351j CCC: $37.00

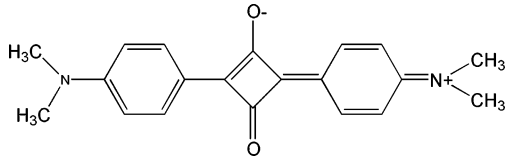

Figure 1. Chemical structure of SQ dye.

we attempted to clarify whether dye molecules encapsulated in SWCNTs can exhibit a photosensitizing function. Recently, we have demonstrated that it is possible to transfer the energy of the excited states of the encapsulated molecule (β-carotene) to the SWCNTs.[17] However, in that case, β-carotene did not act as a photosensitizer because of the overlap of the absorption bands of the encapsulated β-carotene and the SWCNTs. For photosensitization, it is necessary that the absorption band of the encapsulated dye is located in the spectral range where the s-SWCNTs have a low extinction coefficient.

SWCNTs with ~1.4 nm diameter, which was produced with the laser-vaporization method, were used for the dye encapsulation in this study. These tubes can encapsulate C_{60} in high yield.[18] This remarkable characteristic indicates their high purity and open-end structure, both of which are favorable for molecular encapsulation. Squarylium (SQ) dye was chosen for encapsulation into SWCNTs for two reasons: (1) Its absorption does not overlap with the absorption bands of s-SWCNTs with ~1.4 nm diameter. (2) The SQ dye molecule (its chemical structure is shown in Figure 1) is small enough to be encapsulated into the SWCNTs.

The detailed structure of the encapsulated SQ dye was revealed here by X-ray diffraction (XRD) and polarization-resolved optical absorption. Although it is known that high-resolution transmission electron microscopy (HRTEM) can directly probe the encapsulation inside SWCNTs, it is difficult to determine the detailed structure of the encapsulated SQ dye through HRTEM because the electron beam would damage the dye. Thus, we nondestructively studied the structure of the encapsulated SQ dye with the above techniques. Photoluminescence and femtosecond pump−probe measurements clearly revealed that the energy of the excited state of the encapsulated SQ dye is transferred to the SWCNTs. The SQ dye encapsulated SWCNTs (SQ@SWCNTs) could utilize light energies to which pristine SWCNTs were not sensitive. Thus, the encapsulated SQ dye did exhibit the photosensitizing function inside the SWCNTs.

II. Experimental Section

Preparation of SQ Dye and SWCNTs. The SQ dye was synthesized according to the method described in ref 19. The SWCNTs were manufactured through laser vaporization of carbon rods doped with Co/Ni in an argon atmosphere.[18] The SWCNTs were purified with H_2O_2, HCl, and NaOH. The details of the purification procedure have been published previously.[18]

Encapsulation Procedure. The encapsulation of the SQ dye into the SWCNTs was performed as follows. SWCNTs were annealed in air at 350 °C for 20 min just before the encapsulation procedure. SQ dye (30 mg) was dissolved in chloroform (40 mL), and the SWCNTs (1 mg) were added to the solution. The mixture was refluxed for 3 h in N_2 atmosphere in darkness. Next, the solution was filtered and washed with chloroform several times to remove any non-encapsulated SQ molecules. We call the complexes produced in this fashion SQ@SWCNTs. It is important to note that not only SQ dye, but also solvent (CH_3Cl) molecules have been encapsulated into SWCNTs by this procedure as revealed below.

Optical Characterization. Optical absorption spectra were recorded with a commercial Shimadzu spectrophotometer. Thin films of nanotubes were prepared according to the method reported in ref 20. Photoluminescence (PL) mapping was performed with a home-built setup utilizing a tunable Ti-sapphire laser (Spectra-Physics 3900S), or a Xe lamp and a monochromator, for excitation and a single-grating monochromator with an InGaAs diode array for detection. PL measurements were performed on the solutions (1 cm thick silica cells) prepared using the following procedure. Nanotubes were dispersed for 15 min in 1% D_2O solutions of sodium dodecyl−benzene sulfonate (SDBS) using a tip sonifier (20 kHz, power ~40 W). The dispersions were ultracentrifuged for 5 h at 150 000*g*, and the upper 80% supernatant was collected. This supernatant was also used to prepare film samples for polarization-resolved optical absorption. It was 1:1 mixed with 10% water solution of gelatin and cast on Teflon. After drying, films were separated from the substrate, soaked in a 60:40 ethanol:water mixture, and mechanically stretched ~5 times to partially align the SWCNTs to the stretching direction.[21] For Raman measurements, we used a triple monochromator system equipped with a CCD detector (Photon Design Co., PDPT3-640S) and an Ar^+ laser (Spectra Physics, model 2016) operated at 488 nm.

X-ray Diffraction (XRD) Measurements. XRD profiles were recorded using synchrotron radiation with a wavelength of 0.100 nm at the BL1B beam line of the Photon Factory, KEK, Japan. All of the XRD measurements were performed at 330 K in vacuum on powder samples.

Femtosecond (fs) Pump−Probe (PP) Transmittance Measurements. To investigate the relaxation processes following optical excitation of the encapsulated SQ dye, femtosecond pump−probe spectroscopy was applied to the SWCNTs. Two optical parametric amplifiers, excited with a Ti-sapphire regenerative amplifier system (800 nm, 1 kHz), were employed as sources of the pump (708 nm) and probe (1810 nm) pulses. The temporal width and the spectral width of each pulse were 130 fs and 20 meV, respectively, and the time resolution of the system was 190 fs. A change in the transmittance $\Delta T/T$ for the probe pulse induced by the pump pulse was measured as a function of the delay time. The measurements were performed on the thin films of the nanotubes. The absorbance of the SQ@SWCNT film at 708 nm was adjusted to be the same as that of the SWCNT. The intensity of pump pulse was set to be 22 μJ/cm^2.

III. Results and Discussion

XRD Results and Models. XRD measurements can reveal details of the SWCNTs structure, such as degree of intercalation, changes in the arrangement of the SWCNTs (which is denoted here as crystal order), and encapsulation of molecules.[22−26]

(17) Yanagi, K.; Konstantin, I.; Kazaoui, S.; Minami, N.; Miyata, Y.; Maniwa, Y.; Kataura, H. *Phys. Rev. B* **2006**, *74*, 155420−155424.
(18) Kataura, H.; Maniwa, Y.; Kodama, T.; Kikuchi, K.; Hirahara, K.; Suenaga, K.; Iijima, S.; Suzuki, S.; Achiba, Y.; Krätschmer, W. *Synth. Met.* **2001**, *121*, 1195−1196.
(19) Sprenger, H. E.; Ziegenbein, W. *Angew. Chem., Int. Ed. Engl.* **1966**, *5*, 894−894.
(20) Wu, Z.; Chen, Z.; Du, X.; Logan, J. M.; Sippel, J.; Nikolou, M.; Kamaras, K.; Reynolds, J. R.; Tanner, D. B.; Hebard, A. F.; Rinzler, A. G. *Science* **2004**, *305*, 1273−1276.
(21) Kim, Y.; Minami, N.; Kazaoui, S. *Appl. Phys. Lett.* **2005**, *86*, 073103−073105.
(22) Abe, M.; Kataura, H.; Kira, H.; Kodama, T.; Suzuki, S.; Achiba, Y.; Kato, K.; Takata, M.; Fujiwara, A.; Matsuda, K.; Maniwa, Y. *Phys. Rev. B* **2003**, *68*, 041405(R)−0414058.
(23) Maniwa, Y.; Kataura, H.; Abe, M.; Udaka, A.; Suzuki, S.; Achiba, Y.; Kira, H.; Matsuda, K.; Kadowaki, H.; Okabe, Y. *Chem. Phys. Lett.* **2005**, *401*, 534−538.
(24) Liu, X.; Pichler, T.; Knupfer, M.; Fink, J. *Phys. Rev. B* **2003**, *67*, 125403−125410.
(25) Maniwa, Y.; Kumazawa, Y.; Saito, Y.; Tou, H.; Kataura, H.; Ishii, H.; Suzuki, S.; Achiba, Y.; Fujiwara, A.; Suematsu, H. *Jpn. J. Appl. Phys.* **1999**, *38*, 668−670.

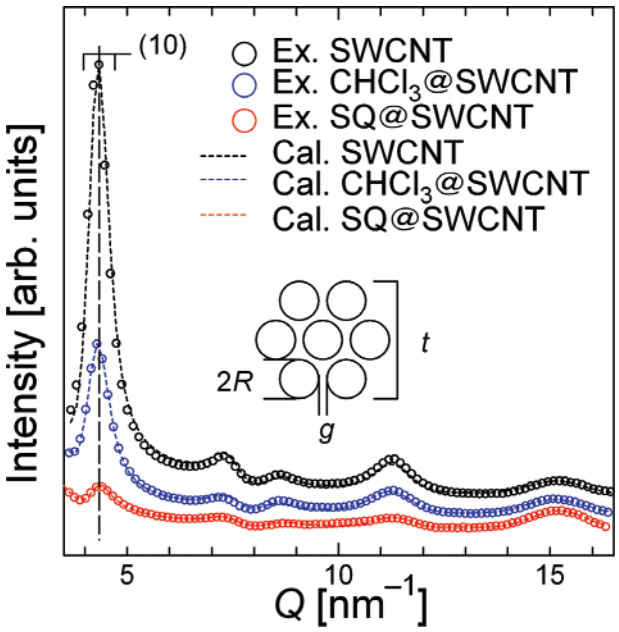

Figure 2. X-ray diffraction profiles of SWCNT (black ○), solvent encapsulated SWCNT ($CHCl_3$@SWCNT, blue ○), and SQ dye encapsulated SWCNT (SQ@SWCNT, red ○). Dotted black, blue, and red lines present the corresponding simulated patterns.

Therefore, XRD is known as one of the most reliable techniques to check whether molecules exist inside or outside SWCNTs. Figure 2 presents the XRD profiles of the initial SWCNT powders, the SWCNTs with encapsulated solvent ($CHCl_3$) molecules, abbreviated as $CHCl_3$@SWCNT, and SWCNTs with encapsulated SQ dye (SQ@SWCNT). The same refluxing and washing treatments have been used for the SQ@SWCNT and $CHCl_3$@SWCNT samples, but with and without SQ dye present, respectively.

The XRD patterns of SWCNTs originate from the diffraction on the two-dimensional triangular lattice of SWCNT bundles and are dominated by the (10) peak.[27] Remarkably, this peak decreased without change in the line width and position upon either solvent or SQ encapsulation. Moreover, the decrease is much stronger in the latter case. If the encapsulation procedure had reduced the crystal order of the SWCNT bundles or had inserted molecules between the SWCNTs (intercalation), then broadening of the (10) peak or/and its shift toward lower Q values would occur,[24] which is not observed in Figure 2. However, encapsulation of molecules inside the SWCNTs naturally explains the observed decrease of the (10) peaks in the $CHCl_3$@SWCNT and SQ@SWCNT samples.[22,23,25,26] To reveal the detailed structure of the encapsulated molecules, numerical simulations were performed as described in refs 22 and 28. In our simulations, the SWCNT walls were simplified as infinitely thin sheets of homogeneous electron density within the carbon covalent networks.

First, we simulated the diffraction on bundles of empty SWCNTs. The SWCNTs with radius R were separated by the distance g and arranged in a bundle of thickness t (see inset in Figure 2), and the radius R was allowed to spread by the value

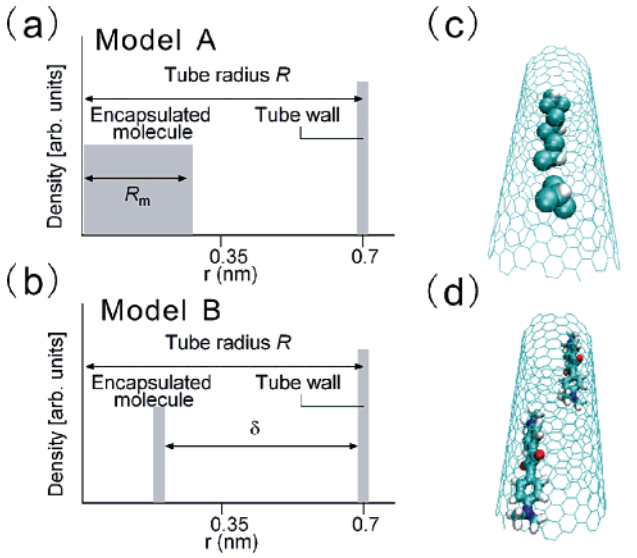

Figure 3. Schematic illustrations of (a) model A and (b) model B used for the analysis of the X-ray diffraction profiles of $CHCl_3$@SWCNTs and SQ@SWCNT powders, respectively, and corresponding structural images: (c) $CHCl_3$ and (d) SQ dye molecules encapsulated in (12,7) SWCNT.

ΔR. This model was successfully fitted into the spectrum of the non-encapsulated SWCNTs (see the dotted black line in Figure 2), yielding the values of $R = 0.69 \pm 0.01$ nm, $\Delta R = 0.06$ nm, $g = 0.32 \pm 0.01$ nm, and $t = 17 \pm 1$ nm, which agree with the previous results of the SWCNTs similar to the tubes used in this study.[22,28] For the analysis of the $CHCl_3$@SWCNT and SQ@SWCNT patterns, the tube diameter, its distribution, the distance between tubes, and the bundle thickness were set to be the same as those of the SWCNTs; that is, a reasonable assumption has been made that those values are not affected by the encapsulation.

The XRD patterns of the $CHCl_3$@SWCNT and SQ@SWCNT powders were reproduced using the following models A and B, respectively. Schematic illustrations of these models are depicted in Figure 3. In model A, the electron density of the encapsulated molecules is located at the center of the tubes and is distributed uniformly within a diameter R_m. The XRD pattern of the $CHCl_3$@SWCNT powder can well be simulated with this model using the following fitting parameters: the weight percent $w = 4.5 \pm 0.2\%$ and $R_m = 0.36 \pm 0.01$ nm. In model B, the electron density of the encapsulated molecules is assumed to be an infinitely thin sheet and located at a distance δ from the tube wall. Figure 2 reveals that model B successfully reproduces the XRD pattern of the SQ@SWCNT system, and the best-fit parameters are $w = 17 \pm 1\%$ and $\delta = 0.42 \pm 0.01$ nm. No acceptable fit of the XRD patterns of the $CHCl_3$@SWCNT and SQ@SWCNT could be achieved in this study with models other than A and B. According to the analysis results for the $CHCl_3$@SWCNT, both solvent and SQ molecules would be encapsulated in the SQ@SWCNT system. The weight percent of SQ dye alone in the SQ@SWCNT system was thus estimated to be approximately 12%.

The above results of the XRD analyses indicate the following two features: (1) The chloroform and SQ molecules are introduced inside, but not outside the SWCNTs. (2) While the chloroform molecules were at the center of the tube, the SQ

(26) Maniwa, Y.; Kataura, H.; Abe, M.; Suzuki, S.; Achiba, Y.; Kira, H.; Matsuda, K. *J. Phys. Soc. Jpn.* **2863**, *71*, 2863−2866.
(27) Tess, A.; Lee, R.; Nikolaev, P.; Dai, H.; Petit, P.; Robert, J.; Xu, C.; Lee, Y. H.; Kim, S. G.; Rinzler, A. G.; Colbert, D. T.; Scuseria, G. E.; Tománek, D.; Fisher, J. E.; Smalley, R. E. *Science* **1996**, *273*, 483−487.
(28) Kadowaki, H.; Nishiyama, A.; Matsuda, K.; Maniwa, Y.; Suzuki, S.; Achiba, Y.; Kataura, H. *J. Phys. Soc. Jpn.* **2005**, *74*, 2990−2995.

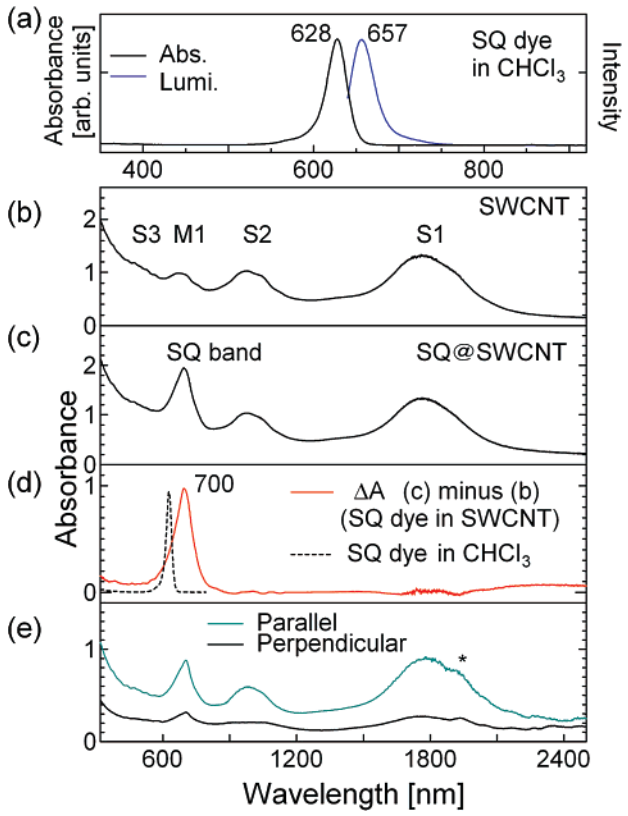

Figure 4. (a) Absorption and luminescence (excitation: 630 nm) spectra of SQ dye in a $CHCl_3$ solution. Absorption spectra of (b) SWCNT and (c) SQ@SWCNT films. (d) Difference absorption spectrum ΔA between the SQ@SWCNT and SWCNT spectra (solid red line). The absorption spectrum of the SQ dye in a $CHCl_3$ solution [dotted black line in (d)] is also shown for comparison. (e) Polarization-resolved absorption spectra from a stretched SQ@SWCNT SDBS/gelatin film. The stretching direction is parallel (top green line) or perpendicular (bottom black line) to the polarization direction of incident light. Asterisk marks a gelatin-related absorption peak.

dye molecules were located at an off-center position inside the SWCNTs. The latter remarkable feature reflects the difference between the chemical structures of the chloroform and the SQ dye molecules. The SQ dye, which has a π-conjugated structure, would exhibit $\pi-\pi$ interactions with the tube wall,[29] and these interactions could shift SQ molecules off the SWCNT center.[29] In contrast, the $CHCl_3$ molecules do not exhibit such interaction with the tube wall and therefore are (uniformly) spread around the center of the tube.

Optical Characterization. Figure 4a shows the absorption and the luminescence spectra of the SQ dye in chloroform. The absorption and luminescence peaks are located at 628 and 657 nm, respectively. Figure 4b shows the absorption spectrum of the SWCNTs. In contrast to the XRD experiments, the chloroform washing procedure, used for the SQ encapsulation, did not affect the optical results. Therefore, non-washed SWCNTs were used as non-encapsulated reference samples. Three absorption bands originating from the three excited states of the s-SWCNTs (S1 1500−2200 nm, S2 800−1200 nm, and S3 400−600 nm) and one from metallic-SWCNTs (M1 600−700 nm) can be clearly identified. The absorption band of the SQ dye falls between the S2 and S3 bands, in the region where the s-SWCNTs have low extinction coefficient; thus the SQ

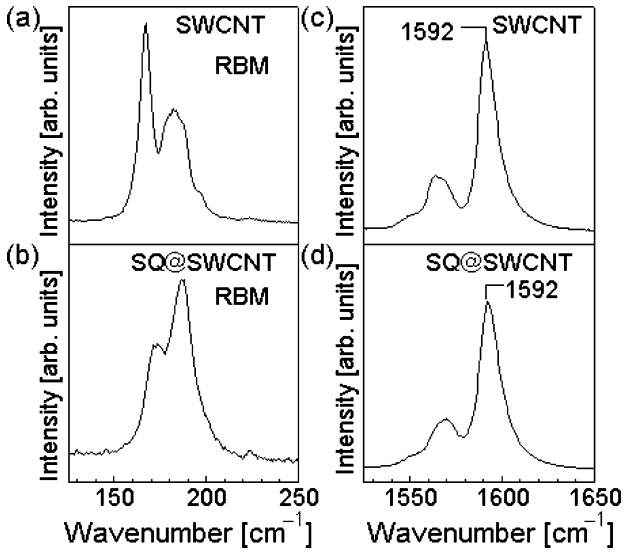

Figure 5. Raman spectra (488 nm excitation) of radial breezing mode (RBM) of (a) SWCNT and (b) SQ@SWCNT powders. The spectra of the G band of (c) SWCNT and (d) SQ@SWCNT are also presented.

dye has the possibility of photosensitizing the SWCNTs. Figure 4c shows the absorption spectrum of the SQ@SWCNT. A new peak, which we label as the SQ band, appeared after the SQ encapsulation. The absorption line shape of the SQ band was clearly identified in the difference absorption spectrum of the SQ@SWCNT and the SWCNT [Figure 4d] spectra. The peak position of the SQ absorption band is red-shifted by 200 meV from that in the solution after the encapsulation, and its line width is broadened from 300 to 900 cm^{-1}. If J-type aggregations occurred, then the line width would decrease.[30] Therefore, such aggregation was not observed in the SQ@SWCNT system. The weight percent w of the encapsulated SQ dye can be roughly estimated as 12% from the absorption intensity of the SQ band. This value is in good agreement with the one derived from the XRD analysis.

Figure 4e presents polarization-resolved absorption spectra from a stretched SQ@SWCNT SDBS/gelatin film, measured with a polarizer set parallel or perpendicular to the stretching direction. The absorption polarization values $\rho = \{(\alpha_{\parallel} - \alpha_{\perp})\}/\{(\alpha_{\parallel} + \alpha_{\perp})\}$ of the SQ band ($\rho = 0.60 \pm 0.01$) were similar to those of S1 ($\rho = 0.64 \pm 0.01$). The alignment of the encapsulated SQ molecules is the same degree as that of the SWCNTs. Thus, the SQ molecules are arranged parallel to the SWCNT axis, as implied above in the XRD analysis. We assume that van der Waals interaction, especially $\pi-\pi$ interaction between the dye and nanotube wall, would be a major force to stabilize SQ dye inside the nanotube.

Figure 5 presents the Raman spectra of the radial breathing (RBM) and G-modes, which are important for the SWCNT characterization, in the SWCNT and SQ@SWCNT powders. As is similarly seen in other molecule-encapsulated SWCNT systems,[9,18] the line shape of the RBM modes changed remarkably through the encapsulation of the SQ dye. It is known that charge transfer between the encapsulated molecules and the SWCNTs decreases the S1 absorption band and causes the peak shift of the G-band.[31] Those changes are not observed for the SQ@SWCNT system [see Figures 4d and 5]. Thus, the lack of

(29) McIntosh, G. C.; Tománek, D.; Park, Y. W. *Phys. Rev. B* **2003**, *67*, 125419−125424.

(30) Tatsuura, S.; Tian, M.; Furuki, M.; Sato, Y.; Pu, L.; Wada, O. *Jpn. J. Appl. Phys.* **2000**, *39*, 4782−4785.

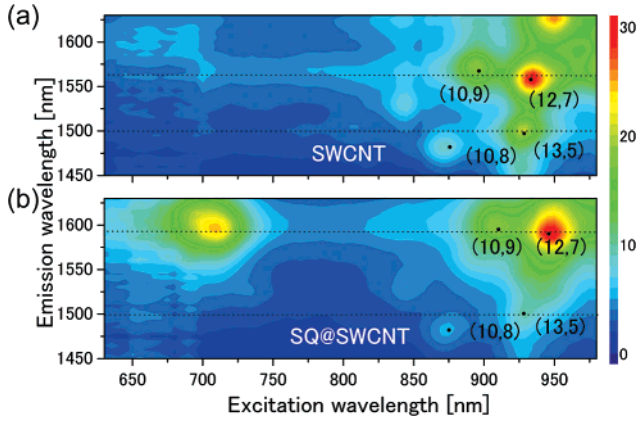

Figure 6. 2D maps of the photoluminescence (PL) excitation/emission peak intensities in (a) SWCNT and (b) SQ@SWCNT in SDBS/D_2O 1% solutions. Dotted lines outline the PL excitation cross-sections shown in Figure 7.

such changes indicates an absence of charge transfer between the SQ dye and SQ@SWCNT.

Photoluminescence Spectra. Figure 6a and b shows 2D maps of the PL excitation and emission peak intensities in the SWCNT and SQ@SWCNT, respectively. Although the luminescence of the SQ dye was completely quenched after the encapsulation, PL signals originating from the nanotubes were easily detected and assigned to the (12,7), (10,9), (13,5), and (10,8) tubes.[32]

The peaks in the PL excitation (PLE) range of 800−1000 nm in Figure 6 originate from excitation into the S2 band followed by emission from the S1 levels. No significant PL signals were observed in the excitation range of 650−750 nm for the SWCNT because the extinction coefficients of the s-SWCNTs are small in this region. However, new PL signals appeared in this region for the SQ@SWCNT sample. These PL signals well correspond to the SQ absorption-S1 emission (see Figure 4). The new PL signals indicate that optical excitation of the encapsulated SQ dye can be transferred to the s-SWCNTs.

Analysis of the PL Maps. In addition to the new PL signals for the SQ@SWCNT system, there are two remarkable features in its PL map: (1) The new PL signals in the region 650−750 nm only appear for the (10,9) and (12,7) tubes, but not for the (10,8) and (13,5) tubes. (2) The positions of PL peaks for the (10,9) and (12,7), but not for the (10,8) and (13,5) tubes, are different between the SQ@SWCNT and SWCNT systems. It is known that high-yield encapsulation of organic compounds can shift the peak positions.[33] Thus, the above observations indicate that the SQ dye was efficiently encapsulated into the (10,9) and (12,7) tubes, but not into the (10,8) and (13,5) tubes. If the SQ molecules were attached outside the tube wall, then the PL signals originating from the dye as well as the shift of the PL peaks would be observed for all of the chiral tubes. Therefore, the observed strong chirality dependence of these features is further evidence for the encapsulation of the SQ dye inside the tubes.

To investigate the PL maps in detail, the PLE spectra of the (10,9) + (12,7) and (10,8) + (13,5) tubes in the SQ@SWCNT and SWCNT samples are plotted in Figure 7. Figure 7c and f

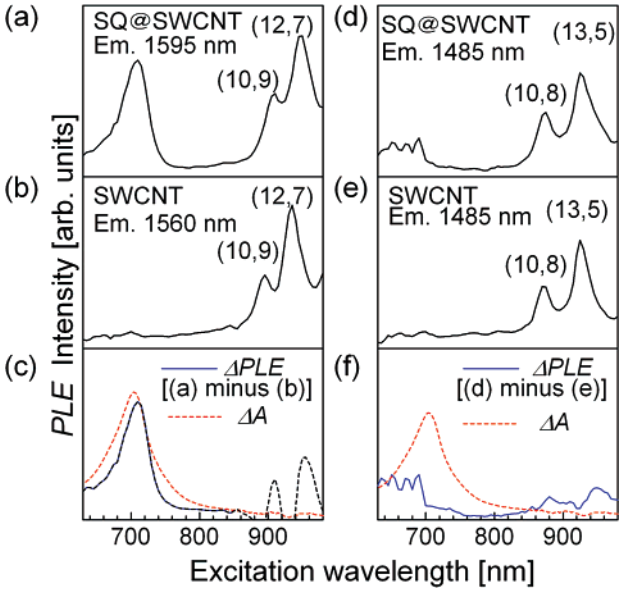

Figure 7. Photoluminescence excitation (PLE) spectra of the (10,9), (12,7), (10,8), and (13,5) tubes in SQ@SWCNT (a and d) and SWCNT (b and e) dispersions. (c) and (f) present the difference PLE (ΔPLE) spectra (blue line) between the SQ@SWCNT and SWCNT spectra. The line shapes of the SQ absorption band (Δ*A*, dotted red line), which is derived from the difference between the absorption spectra of the SQ@SWCNT and SWCNT, are shown for comparison in (c) and (f).

presents the corresponding difference PLE (ΔPLE) spectra between the SQ@SWCNT and SWCNT samples. The line shapes of the SQ absorption band, which is derived from the difference between the absorption spectra of the SQ@SWCNT and SWCNT samples, are also shown in (c) and (f) for comparison. ΔPLE line shape that is similar to the line shape of the SQ absorption band is clearly seen in the (10,9) and (12,7) tubes, but not in the (10,8) and (13,5) tubes. The (10,9), (12,7), (10,8), and (13,5) tubes have diameters of 1.31, 1.32, 1.24, and 1.28 nm, respectively. Thus, this result might indicate that a diameter threshold of ∼1.3 nm exists for the encapsulation of SQ dye into SWCNTs.

Precise determination of the quantum yield of the energy transfer from the encapsulated dye to SWCNTs is difficult because of the following reason: As is shown in Figure 7, emission intensity caused by the energy transfer from SQ dye strongly depends on the tube chirality. Therefore, it is necessary to clarify the absorbance of the dye encapsulated in a single chiral tube for the correct evaluation of the quantum yield, and it is, unfortunately, quite difficult to identify such absorbance. As a rough estimation, the quantum yield is expected to be quite high, because the absorbance of encapsulated dye is similar to that of the S2 band (Figure 4) and the emission intensity after photoexcitation of SQ dye is almost the same as that by direct excitation of the S2 band (Figure 7a).

Relaxation Dynamics of Photoexcited SQ@SWCNT System. In the previous section, the presence of the energy transfer from the encapsulated SQ dye to the SWCNT was revealed by the PL measurements. The following energy transfer pathway was assumed. The photon energy absorbed by the SQ dye was transferred to the S2 band of SWCNT, and then internally relaxed to the S1 band, and finally the emission from the S1 band was observed (Figure 8). The excited-state energy of the encapsulated SQ dye after its photoexcitation is ∼1.7 eV. This energy can be transferred to the SWCNT S2 band extending

(31) Kavan, L.; Rapta, P.; Dunsch, L.; Bronikowski, M. J.; Willis, P.; Smalley, R. E. *J. Phys. Chem. B* **2001**, *105*, 10764−10771.
(32) Weisman, R. B.; Bachilo, S. M. *Nano Lett.* **2003**, *3*, 1235−1238.
(33) Li, L.; Khlobystov, A. N.; Wiltshire, J. G.; Briggs, G. A.; Nichlolas, R. J. *Nat. Mater.* **2005**, *4*, 481−485.

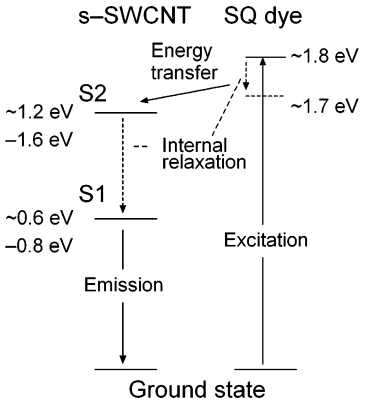

Figure 8. Schematic illustration of the energy relaxation pathway after photoexcitation of the SQ dye encapsulated in semiconducting-SWCNTs (s-SWCNT) with ~1.4 nm diameter. The energy diagrams are depicted in the exciton picture.

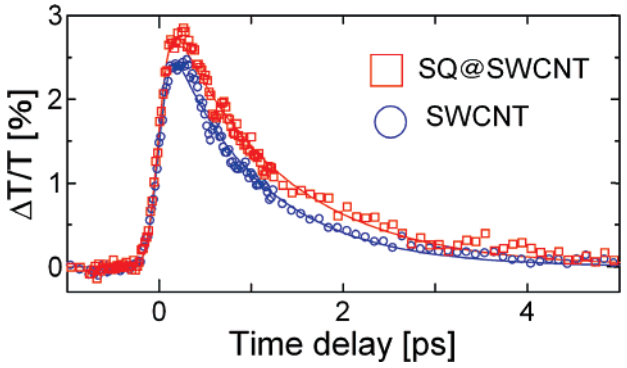

Figure 9. Transient transmittance change of the S1 absorption (at 1810 nm) after 708 nm photoexcitation of SWCNT (bottom blue ○) and SQ@SWCNT (top red □) films. Solid red and blue lines are the simulation results for SQ@SWCNT and SWCNT, respectively, using monoexponential functions convoluted with the system response.

from 1.2 to 1.6 eV with a concomitant emission of multiple phonons. According to this energy transfer pathway, strong excitation of the encapsulated SQ dye could lead to the saturation of the S1 absorption band.

Previous femtosecond pump−probe (PP) measurements, which were performed on bundles of metallic and semiconducting SWCNTs, have revealed the absorption saturation of the S1 band after photoexcitation of higher-energy bands of SWCNTs.[34−36] The films used for the PP measurements in this study are similar to the ones used for those measurements.[34−36] If the energy of the excited states of SQ dye were transferred to the S1 band, then an enhancement of the absorption saturation of the S1 band would be observed. With reference to those measurements, to clarify the relaxation process after the photoexcitation of the encapsulated SQ dye, we performed the PP measurements on the SQ@SWCNT and SWCNT films. The absorption spectra of the films are similar to those shown in Figure 4; however, the absorbance at the wavelength of pump pulse, 708 nm, of the SQ@SWCNT film was adjusted to be the same as that of the SWCNT.

Figure 9 shows the changes in transmittance as a function of time delay at the peak position of the S1 band, 1810 nm, after 708 nm excitation of the SWCNTs and SQ@SWCNTs films. The dynamics can be well simulated using monoexponential functions convoluted with the system response. As is consistent with the previously reported results,[34−36] the dynamics with a decay time constant of about 1 ps was observed in the both samples. Although the light-intensity absorbed by the SQ@SWCNT sample at the pump wavelength was the same as that by the SWCNT, there is a significant (15%) enhancement of the saturated absorption in the SQ@SWCNT sample, thus clearly indicating that energy transfer occurred from the encapsulated SQ dye to the SWCNTs. This enhancement is not as large as the changes observed in PL measurements. The presence of nanotube bundling in the samples for the PP measurements would reduce the saturated absorption change because the bundling strongly increases intertube interactions that induce the energy transfer from semiconducting to metallic nanotubes.

(34) Lauret, J.-S.; Voisin, C.; Cassabois, G.; Delalande, C.; Roussignol, P.; Jost, O.; Capes, L. *Phys. Rev. Lett.* **2003**, *90*, 057404−057407.
(35) Korovyanko, O. J.; Sheng, C.-X.; Vardeny, Z. V.; Dalton, A. B.; Baughman, R. H. *Phys. Rev. Lett.* **2004**, *92*, 017403−017406.
(36) Maeda, A.; Matsumoto, S.; Kishida, H.; Takenobu, T.; Iwasa, Y.; Shiraishi, M.; Ata, M.; Okamoto, H. *Phys. Rev. Lett.* **2005**, *94*, 047404−047407.

We could not detect any difference in the rise time between SWCNT and SQ@SWCNT films. This result indicates that the energy of the excited states of the encapsulated SQ dye is transferred to the SWCNTs within the time resolution (190 fs) of our system.

IV. Conclusions

Squarylium (SQ) dye was successfully encapsulated in SWCNTs to expand the light spectrum that can be utilized by the nanotubes. The photosensitive function of the encapsulated dye was clearly observed. X-ray diffraction revealed that the dye molecules were efficiently encapsulated at off-center positions inside the tubes. Polarization-resolved absorption revealed that the dye molecules are aligned to the SWCNT axis. Raman scattering indicated the absence of the charge transfer between the encapsulated dye and the SWCNTs. Photoluminescence spectra revealed efficient energy transfer from the encapsulated dye to the SWCNTs. The filling rate of the SQ molecules strongly depends on the nanotube diameter. The femtosecond pump−probe transmittance measurements clarified the enhancement of the saturated absorbance of the S1 band after the photoexcitation of the encapsulated SQ dye. Ultrafast energy transfer from the encapsulated SQ dye to the SWCNTs was revealed. Dye encapsulated SWCNTs can utilize a wider light spectrum than pristine SWCNTs; that is, the encapsulated dye does exhibit a photosensitization function. The techniques reported here should open the way to manipulating the optical properties of SWCNTs through the encapsulation of organic compounds.

Acknowledgment. We are thankful for a Grant-in-Aid from the Foundation Advanced Technology Institute, The Sumitomo Foundation (Grant No. 050645), and JSPS.KAKENHI [18740187 (K.Y.), 18201017 (H.K.)].

Supporting Information Available: Changes of absorbance of SQ dye encapsulated in SWCNTs and dispersed in a poly methyl methacrylate (PMMA) polymer through a heating process in air. This material is available free of charge via the Internet at http://pubs.acs.org.

JA067351J